Technical Paper

ISSN 1997-1400 Int. J. Pavement Res. and Technol. 1(4):143-147

Influence of Concrete Joints on Roughness Index and Pavement Serviceability

Chiu Liu[1+], Zhongren Wang[2], and James N. Lee[3]

Abstract: Pavement joints may cause strong vibrations in moving vehicles discomforting or annoying drivers and passengers at times. Conventionally, two important indices, International Roughness Index (*IRI*) and Present Serviceability Index (*PSI*) have been chosen to characterize pavement ride quality. Increase of *IRI* and reduction of *PSI* in the presence of pavement joints are analytically derived by employing a vehicle model across joints of different geometries. The dependence of ride quality reduction on joint width, vertical fault, and tire-road contact length are explicitly derived. Theoretical predictions agree well with the Federal Highway Administration (FHWA) reported data. These research results are important for maintaining pavement systems and possibly for establishing pavement quality control criterion.

Key words: *Concrete joints; Fault; International roughness index; Joint width; Ride quality; Serviceability; Vehicle.*

Introduction

Ride quality, characterized by present serviceability index (*PSI*), was introduced into pavement design in the American Association of State Highway and Transportation Officials (AASHTO) road test [1-5]. In the early 1980s, the international roughness index (*IRI*) was proposed to be an indicator of pavement roughness and ride quality for highways [6, 7]. Although pavement ride quality is mainly determined by the jerk intensity experienced by passengers in moving vehicles [8], *IRI* was adopted in many countries as a ride quality and a roughness standard [9-11]. Moreover, *IRI* was used as an overall pavement performance indicator [12-15] and further related with pavement test methods and specification [16]. Furthermore, it has been applied as a network level performance indicator [17, 18], a standard for smoothing pavement surfaces [19], a tempted measure of bridge ride quality [20], and a ride quality standard for urban streets [21].

Because concrete joints may substantially increase the *IRI* [22-24] and intensify vehicle-road dynamic interaction [25, 26], investigating the influence of joints on *IRI* in jointed concrete pavements (JCP) has attracted much attention lately. Driving on a JCP can be annoying because an uneven joint causes a passenger experiencing vibration at least twice when vehicle tires come into contact successively with the joint. Since a one lane-mile JCP section is constructed by joining about 320 slabs, a passenger seated in a car traveling at 96kph (60mph) will feel 640 pulses per minute. The unevenness although initially small, might have been introduced during pavement construction. Saw cuts with a width from 3.3mm to 6.4mm are performed on slabs to create joints as they are cured; and the cuts aren't and perhaps won't be made perfect along all wheel paths. Thus, limiting joint faults within a defined range can be crucial to extend pavement serviceable life and to control pavement construction quality. The immediate question is how one can quantitatively relate the uneven joints to the pavement roughness and ride conditions. Based on a vehicle model, equations for ride quality *PSI* and roughness index *IRI* will be derived by considering vehicle dynamics, slab sizes, and different joint geometries.

Because low *PSI* or high *IRI* may accelerate pavement deterioration, the effect of both joint width and fault depth on pavement roughness and ride quality is investigated. The dynamic vehicle-road interaction is quantitatively assessed using the known quarter car model (see Fig. 1), which has been successfully applied to understand vehicle vibration on roads of various profiles [25-27].

Formulation

Consider a vehicle moving over concrete joints shown in Fig. 2 along a given direction. In order to pin point the vibration due to joints only, the concrete pavement surface is assumed to be flat first; and the vibration induced by a rough profile can always be added on later. Thus, the road profile appears to be smooth everywhere except at the joints in between two adjacent slabs. Denoting the displacements from the equilibrium positions of the sprung mass and the unsprung mass as $z_s(x)$ and $z_u(x)$, and the surface profile by $z(x)$, one can describe the vertical dynamic vibrations of the quarter vehicle [8] by:

$$M_s\ddot{z}_s + k_s(z_s - z_u) + c_s(\dot{z}_s - \dot{z}_u) = 0 \tag{1}$$

$$M_s\ddot{z}_s + M_u\ddot{z}_u + c_t(\dot{z} - \dot{z}_u) = k_t(z - z_u) \tag{2}$$

Shown in Fig. 1 are a sprung mass M_s rested on top of an unsprung mass M_u through a spring with elastic constant k_s and a dashpot with a viscous parameter c_s. Constant k_t and the viscous parameter c_t characterize tire mechanical property. A road profile characterized by a spatial period of $\tilde{L} = 2L_1$ can be expanded in terms of a Fourier series, namely:

[1] California Department of Transportation, PhD, PE, TE, 1120 N Street, MS-36, Caltrans/HSIP, Sacramento, CA 95814, USA.
[2] Senior Engineer, Caltrans/Traffic Operation, 1120 N Street, MS-36, Sacramento, CA 95814, USA.
[3] Pavement Engineer, Transportation Research Laboratory, 5900 Folsom Blvd, MS-5, Sacramento, CA 95819, USA.
[+] Corresponding Author: E-mail Chiu_Liu@dot.ca.gov
Note: Submitted January 1, 2008; Revised May 12, 2008; Accepted June 9, 2008.

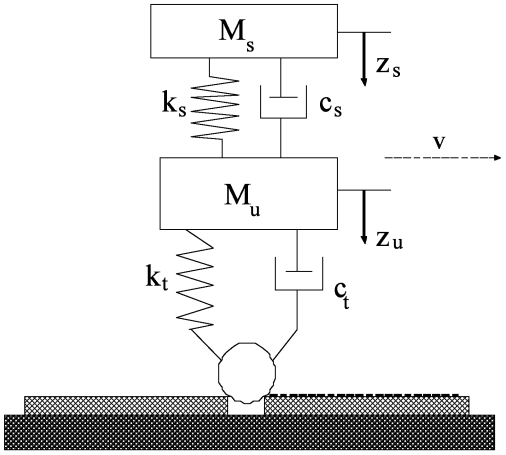

Fig. 1. Sketch of a Moving Quarter Vehicle.

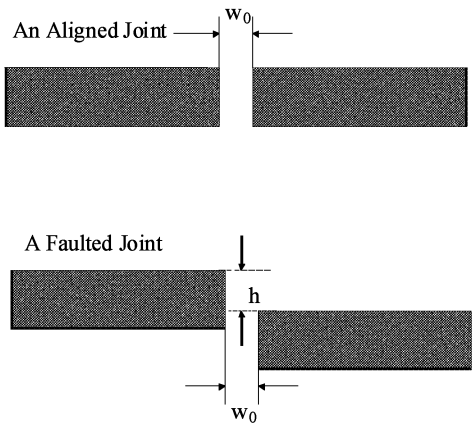

Fig. 2. Sketch of Two Types of Concrete Joints.

$$z(x) = A_0 + \mathrm{Re}\sum_{n=1}^{\infty} A_n e^{-i\phi_n + i2n\pi x/\tilde{L}} \tag{3}$$

$$A_n\cos\phi_n = \frac{2}{\tilde{L}}\int_0^{\tilde{L}} z(u)\cos(2n\pi u/\tilde{L})du,\ A_n\sin\phi_n = \frac{2}{\tilde{L}}\int_0^{\tilde{L}} z(u)\sin(2n\pi u/\tilde{L})du \tag{4}$$

The expansion coefficient A_n is real quantity, ϕ_n is a phase angle, and the integer $n \geqq 1$. Constant A_0 isn't of any concerns because it solely vertically shifts the measurement reference plane, i.e. the x-axis. The vertical displacement $z_u(x)$ of the unsprung mass and $z_s(x)$ the sprung mass for Eqs. (1) and (2) are found via Eq. (3)

$$z_u(x) = \mathrm{Re}\left\{\sum_{n=1}^{\infty} A_n \frac{(k_s - M_s\omega_n^2 + i\omega_n c_s)(k_t - i\omega_n c_t)}{\Theta} e^{i\omega_n t - i\phi_n}\right\} \tag{5}$$

$$z_s(x) = \mathrm{Re}\left\{\sum_{n=1}^{\infty} A_n \frac{(k_s + i\omega_n c_s)(k_t - i\omega_n c_t)}{\Theta} e^{i\omega_n t - i\phi_n}\right\} \tag{6}$$

$$\Theta = (k_t - M_u\omega_n^2 - i\omega_n c_t)(k_s - M_s\omega_n^2 + i\omega_n c_s) - M_s\omega_n^2(k_s + i\omega_n c_s) \tag{7}$$

where angular frequency $\omega_n = 2n\pi v/\tilde{L}$, and the vehicle moving position x is substituted for convenience by 'vt'. In addition, the vehicle parameters are set according to k_s/M_s = 62.3, k_t/M_s = 653, m_u/M_s = 0.15, c_t/M_s = 0.1, and c_s/M_s = 6.0 [6]. The jerk relative to ground, namely the rate of change of acceleration experienced by riders, is found by differentiating Eq. (6) against time 't' repetitively for three times.

$$J_s(t) = -\mathrm{Re}\left\{\sum_{n=1}^{\infty} A_n \frac{i(k_s + i\omega_n c_s)(k_t - i\omega_n c_t)\omega_n^3}{\Theta} e^{i\omega_n t - i\phi_n}\right\} \tag{8}$$

Eq. (8) is a periodic function of time with a period T equal to $\tilde{L}/v$. Within a moving vehicle, a rider is sensitive to the jerk intensity, which matches with the variance of the jerk when it is considered approximately a random variable [28].

$$\sigma_J^2 = \frac{1}{T}\int_0^T J_s(t) \times J_s^*(t)dt \tag{9}$$

or

$$\sigma_J^2 = \sum_{n=1}^{\infty} \omega_n^6 A_n^2 (k_s^2 + \omega_n^2 c_s^2)(k_t^2 + \omega_n^2 c_t^2)/2\Theta\Theta^* \tag{10}$$

Symbol Θ^* is the complex conjugate of Θ. Eq. (10) relates the road profile spectrum and vehicle mechanical characteristics to the vibration environment inside a moving vehicle. The jerk intensity is directly related to a ride quality index (RQI), such as *PSI*, ride index (RI), mean panel index (MPI), etc via a proposed equation [8]:

$$PSI = 5 - \beta \times \log\left(\sigma_J / \sigma_{J,0}\right) \tag{11}$$

where quantity β is determined to be around 2.80. Quantity $\sigma_{J,0}$ depending on measurement devices reflects the human sensitivity threshold for jerk. Using Eqs. (5) and (6), one can express the *IRI* by [28]:

$$IRI = \frac{1}{vT}\int_0^T \left|\dot{z}_s(t) - \dot{z}_u(t)\right| dt \tag{12}$$

Where speed v, kept at 80kph (50mph), is the cruise speed of a measurement vehicle. When time derivative of the relative displacement, i.e. $\dot{z}_s - \dot{z}_u$, is random, Eq. (12) is transformed to

$$IRI = \frac{1}{v}\sqrt{\frac{1}{\pi}}\left\{\sum_{n=1}^{\infty} \frac{M_s^2\omega_n^6 A_n^2 (k_t^2 + \omega_n^2 c_t^2)}{\Theta\Theta^*}\right\}^{1/2} \tag{13}$$

Joints without Vertical Fault

Only a brief summary and examples of the test results are presented in this paper. A complete list of all test results including binder and mix parameters can be found in the technical report submitted to the NCHRP [2].

$$z \cong \begin{cases} -w_0^3/(24Rw_c) & 0 \leq x \leq w_c \\ 0 & w_c < x \leq L + w_0 \end{cases} \tag{14}$$

where quantities L, R, w_0, and w_c represent the slab length, radius of a tire, joint width, and tire-road contact length, respectively. The spatial period $\tilde{L}$ of the pavement profile $z(x)$ for joints without fault is equal to $L + w_0$. Using Eq. (4), the coefficient A_n for each

sinusoidal component of a profile is computed to be

$$A_n = \frac{w_0^3}{24R\tilde{L}}\{(\sin\varphi_n/\varphi_n)^2 + [(1-\cos\varphi_n)/\varphi_n]^2\}^{1/2} \quad (15)$$

$$\phi_n = \varphi_n/2 = n\pi w_c/\tilde{L} \quad (16)$$

Substituting Eq. (15) into Eq. (10) yields

$$\sigma_J = (v^3 w_0^3/24\tilde{L}Rw_c^3)\times\sqrt{\sum_{n=1}^{\infty} R_n^2 a_n^2 \varphi_n^6/2} \quad (17)$$

$$R_n^2 = (k_s^2+\omega_n^2 c_s^2)(k_t^2+\omega_n^2 c_t^2)/\Theta\Theta^*$$

$$a_n^2 = (\sin\varphi_n/\varphi_n)^2 + [(1-\cos\varphi_n)/\varphi_n]^2 \quad (18)$$

The jerk intensity increases cubically with the width and the vehicle moving speed respectively. Applying Eq. (11), the reduction of *PSI* can be derived

$$\Delta PSI \cong 2.80\times\log(\sigma_J/\sigma_{J,0}) \quad (19)$$

The threshold $\sigma_{J,0}$ was determined to be in the neighborhood of $0.33 m/s^3$ [8]. Using Eq. (14) and assuming a tire radius of 0.32m (12.5inches) and contact length of 0.10m (4inches), the maximal change of road profile across a joint is estimated to be approximately 2.6μm for a 12.5mm (0.5inches) joint width. The jerk intensity caused by a flat joint goes beyond the threshold (~$0.33 m/s^3$) only when joint width becomes wider than approximately 1.9cm (0.75inches). Thus, when both sides of a joint are aligned, the vibration induced by joint width is little practical significance, especially for newly constructed pavements. It is expected that the height of faulting will develop across a joint as the joint deteriorates. Let's turn attention to joints with vertical fault, a common situation found in almost all pavements.

Joints with Vertical Fault

The road profile $z(x)$ can be approximated by rolling a wheel across the joint with enveloping effect taken into account; and at the joint, $z(x)$ represents the vertical displacement of the wheel center. Profile $z(x)$ repeats itself with a period of $2(L+w_0)$ with one downward fault and the other upward fault, yielding,

$$z(x) \cong \begin{cases} h(1-2x/w_c)/2 & 0 \le x < w_c \\ -h/2 & w_c \le x < L_1 \\ -h[1-2(x-L_1)/w_c]/2 & L_1 \le x < L_2 \\ h/2 & L_2 \le x < 2L_1 \end{cases} \quad (20)$$

where quantity h represents the magnitude of the vertical fault at joints; and lengths L_1 and L_2 are respectively equal to $L+w_0$ and $L+w_0+w_c$. It is further assumed that $h<<R$ and $w_0<<w_c$. These two conditions are well satisfied by noting that both the joint width and the vertical fault are in the order of 1cm or less, and the radius of a vehicle tire is around 0.406m (16inches). Fourier coefficients for various components of the profile $z(x)$ given by Eq. (20) are derived as

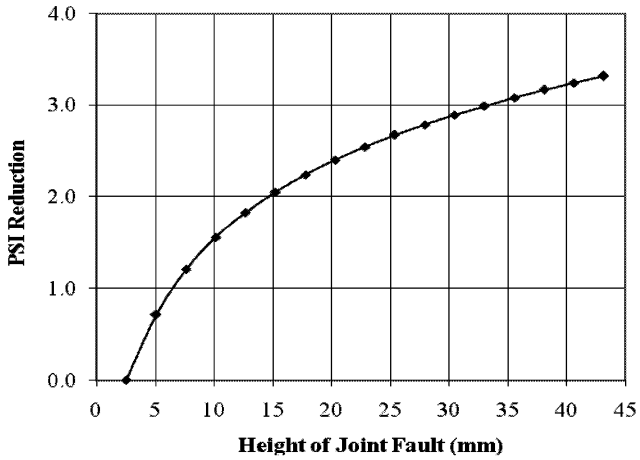

Fig. 3. Serviceability or Ride Quality Reduction Plotted against Depth of Joint Fault.

$$A_n = hw_c(a_n^2+b_n^2)^{1/2}/2 \quad (21)$$

Where

$$a_n = [-\sin\varphi_n/\varphi_n + 2(1-\cos\varphi_n)/\varphi_n^2]\times[1+(-1)^{n-1}]$$

$$b_n = [-2\sin\varphi_n/\varphi_n^2 + (1+\cos\varphi_n)/\varphi_n]\times[1+(-1)^{n-1}]$$

$$\phi_n = \tan^{-1}(b_n/a_n) \in (-\pi,\pi)$$

Using Eq. (10), the jerk intensity in a moving vehicle is estimated to be

$$\sigma_J \cong (v^3 h/2\tilde{L}w_c^2)\times\sqrt{\sum_{n=1}^{\infty} R_n^2(a_n^2+b_n^2)\varphi_n^6/2} \quad (22)$$

It can be inferred from Eq. (22) that the jerk intensity experienced by drivers is proportional to the vertical fault of the joint, and approximately proportional to the cubic of the vehicle moving speed. This holds so long as the vertical fault h is above certain limit, namely, when $h > h_{\min} = w_0^3/24Rw_c$. A typical value for $h_{\min}$ is found to be approximately 2.1μm by assuming parameters R, w_c, and w_0 to be 0.32m, 0.127m, and 0.0127m, respectively. It points out the fact that the jerk intensity doesn't vanish although small for an almost perfectly aligned joint. From a practical standpoint, Eq. (22) is always valid because when a wheel is about to cross a joint, a transient vertical fault greater than a few micrometers can be induced. Plotted in Fig. 3 is the reduction of ride quality *PSI* against the height of the fault, where the R, L, w_c, h, and v are assumed to be 0.32m (12.5inches), 6.10m (20ft), 0.127m (5inches), 1.27cm (0.5inches), and 24.7m/s (55mph), respectively. The fault depth perhaps should be controlled below 2.0mm for new pavements. Once the vertical fault approaches 1.25cm, the reduction in *PSI* will degrade a pavement section down to an unacceptable service level. The fault depth should be controlled below several millimeters during pavement life in order to enhance pavement performance.

Using Eq. (13), the *IRI* in a moving vehicle is derived to be

$$IRI = (v^2 h/2\tilde{L}w_c^2)\times\sqrt{\sum_{n=1}^{\infty}\tilde{R}_n^2(a_n^2+b_n^2)\varphi_n^6/2} \quad (23)$$

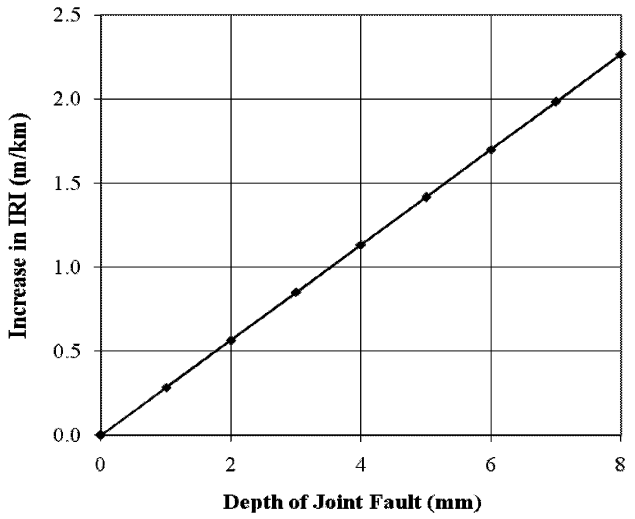

Fig. 4. Increase of *IRI* Plotted against Depth of Joint Fault.

where $\tilde{R}_n^2 = M_s^2(k_t^2 + \omega_n^2 c_t^2)/\Theta\Theta^*$. It is important to note that the *IRI* is proportional to the vertical fault; but one should be careful not to say that the *IRI* depends on speed *v* because *IRI* is measured at the fixed speed of 80kph (50mph). Eq. (23) holds in general because the vertical fault *h* is practically greater than $h_{\min}$, usually in the order of a few micrometers. Plotted in Fig. 4 is the increase of *IRI* for a joint width of 6.4mm against the vertical fault in units of millimeters. The slope of the increasing *IRI*, depending on the dynamic characteristics of measurement vehicles, isn't universal. The slope in the figure is approximately 0.3m/mm, in agreement with some of the reported data [29, 30]. The *R*, *L*, w_c, w_0, and *v* are respectively assumed to be 0.32m, 7.6m, 0.152m, 6.4mm, and 22.3m/s. Once the vertical fault reaches about 10mm, the increase in *IRI* indicates the concrete pavement is at its late stage of serviceable life.

How can *IRI* and σ_J be evaluated when the fault depth isn't uniform but random for a pavement with M number of joints? In this case, both *IRI* and σ_J are found to be

$$IRI = \sqrt{\sum_{i=1}^{M} IRI_{J_i}^2} \tag{24}$$

$$\sigma_J = \sqrt{\sum_{i=1}^{M} \sigma_{J_i}^2} \tag{25}$$

where jerk intensity σ_{J_i} and index IRI_{J_i} due to the *i*-th joint are evaluated using Eqs. (22) and (23) with a fault depth of h_i and a spatial period $\tilde{L}$ equivalent to the length of the entire road profile under consideration. Note that the predictions made using Eqs. (12), (13), (23), and (24) in general differ from the measured *IRI* using a profiler [9]; however, they are offset by a calibration value, and the correlation between the theoretical predicted *IRI* and the measured *IRI* was found nearly 100% [8, 28].

Joints Embedded along a Road Profile

In this situation, the question is what would be the reduction in *IRI* or increase of *PSI* when the joints were smoothed out along a road with an arbitrary profile? Lets used the subscripts '*m*', '*s*', and '*o*' to indicate an quantity that is measured in the presence of untreated joints with faults, measured in the presence of smoothed joints, and measured when the road is almost perfectly smooth with untreated joint faults, respectively. Both the increase of *PSI* and decrease of *IRI* when joints are smoothed can be estimated via

$$IRI_s = \sqrt{IRI_m^2 - IRI_o^2} \tag{26}$$

$$\Delta PSI_s = \sqrt{\Delta PSI_m^2 - \Delta PSI_o^2} \tag{27}$$

Note that both ΔPSI_o and IRI_o can be calculated using Eqs. (10), (13), (22), and (23) or evaluated using empirical equations derived from a set of temporal profile data for a given road segment. For example, let say IRI_o = 1.0m/km, IRI_m = 1.5m/km, then smoothing the joints will reduce the *IRI*, yielding $IRI_s \approx$ 1.1m/km, which decreases substantially the IRI_m for unsealed joints. Similar inference can be made to the ride quality.

Conclusions

In this investigation, we have estimated the influence of concrete joints on ride quality and roughness index *IRI*. It is found that predictions derived from the analytic model are in good agreement with data collected by FHWA [2, 29] and the computing program in use [30], showing the importance of the model for guiding both field practices and future research. If all joints were well aligned, the reduction in ride quality and the increase in *IRI* might be practically negligible when joint width is small. However, a transient fault may be induced when a wheel approaching a perfectly aligned joint. Most joints are presented with vertical faults in reality; and the reduction in ride quality and the increase of *IRI* may become significantly large. Thus, minimizing or controlling the vertical faults of joints in a few millimeters range is important to enhance the ride quality, substantially reduce the roughness index, and lower dynamic wheel loads across pavement joints. Diamond grinding over joints and joint sealing are often employed in the past to smooth pavement profiles. Nevertheless, it is important for engineers to know when such maintenance should be done in order to substantially extend the pavement serviceable life.

References

1. American Association of State Highway and Transportation Officials (AASHTO), (1993). *AASHTO Guide for Design of Pavement Structures*, Washington D. C., USA.
2. National Cooperative Highway Research Program (NCHRP), (2001). Guide for Empirical Pavement Design, Appendix 00-1: Background and Preliminary Smoothness Prediction Models for Flexible Pavement, *NCHRP Report, No.1-37,* Feb, Transportation Research Board, National Research Council, Washington D. C., USA.
3. Baus, R.L. and Wang, W., (2004). Development of Profiler-Based Rideability Specifications for Asphalt Pavements and Asphalt Overlays, *FHWA, Report SC-04-07.*
4. Liu, C. and Herman, R., (1996). New Approach to Roadway Performance Index, *J. Transp. Eng.*, **122**(5), pp. 329-336.

5. Smith, K., Zimmerman, K., and Finn, F., (2004). AASHTO Road Test-the Living Legacy for Highway Pavements, *TR NEWS,* Vol. 232**,** pp. 14-24.
6. Sayers, M.W., Gillespie, T.D., and Quieroz, C.A.V., (1986). The International Road Roughness Experiments, *World Bank Tech. Report*, Vol. 45, pp. 23.
7. Liu, C., (2000). Vehicle-Road Interaction, Evolution of Road Surface Profiles and Present Serviceability Index, *International Journal of Road Materials and Pavement Design,* **1**(1), pp. 35-51.
8. Liu, C. and Herman, R., (1999). Roadway Profile, Vehicle Dynamics, and Ride Quality Rating, *J. Transp. Eng.*, **125**(2), pp. 123-128.
9. Gillespie, T.D., Sayers, M.W., and Segel, L., (1980). Calibration of Response-Type Road Roughness Measuring System, *NCHRP Report*, *No. 228*, Transportation Research Board, National Research Council, Washington D. C., USA.
10. Rauhut, J.B., Eltahan, A, and Simpson, A.L., (1999). Common Characteristics of Good and Poorly Performing AC Pavements, *FHWA-RD-99-193, FHWA*, Washington D.C., USA.
11. Liu, C. and Wang, Z., (2006). Physical Characterization of Pavement Profile and Ride Quality: Past, Present, and Future, *Shanghai Highways, an International Journal*, **1**(99), pp. 7-9.
12. Yew, C. and Friedman, P., (2002). Measuring the Road to Improvement, *Public Roads,* USDOT and FHWA, **66**(3), pp. 18-22.
13. Hansen, K., (2004). Pavement Preservation through Prevention, *HMAT* (NAPA), **9**(3), pp. 23-26.
14. Delanne, Y. and Pereira, P.A.A., (2001). Advantages and Limits of Different Road Roughness Profile Signal-Processing Procedures Applied in Europe, *Transp. Res. Rec.*, *No. 1764*, pp. 254-259.
15. Kawamura, A., Takahashi, M., and Inoue, T., (2001). Basic Analysis of Measurement Data from Japan in Even Project, *Transp. Res. Rec.*, *No. 1764*, pp. 232-242.
16. Killingsworth, B., (2004). Quality Characteristics and Test Methods for Use with Performance Related Specification of Hot Mixed Asphalt Pavements, *NCHRP, Report No.9-15*, Transportation Research Board, National Research Council, Washington D. C., USA.
17. Li, N., Kazmierowski, T., and Shaema, B., (2001). Verification of Network-Level Pavement Roughness Measurements, *Transp. Res. Rec.*, *No. 1764*, pp. 128-138.
18. Lu, J.J., Zhu, C., and Pernia, J., (2003). Performance Evaluation of Roughness Measuring Devices To Measure Ride Number And International Roughness Index, *Final Technical Report*, Department of Civil and Environmental Engineering, University of South Florida, Tampa, FL., USA.
19. Mccandless, P., (2001). Tailoring to the Pants: Penn DOT Works Smoothness into $700 Million I-99 Corridor, *Roads and Bridges*, **39**(10), pp. 32-35.
20. Mcghee, K.K., (2002). A New Approach to Measuring the Ride Quality of Highway Bridges, *FHWA/VTRC Report 02-R10,* FHWA, Washington D. C., USA.
21. Shafizadeh, K. and Mannering, F., (2003). Acceptability of Pavement Roughness on Urban Highways by Driving Public, *Transportation Research Record, No. 1860*, pp. 187-193.
22. Corley-Lay, J. and Mossison, C.S., (2002). Thirty-Three-Year Performance of Jointed Concrete Test Sections in North Carolina, *Transp. Res. Rec.*, *No. 1806*, pp. 88-94.
23. Felker, V., Najjar, Y.M., and Hossain, M., (2004). Modeling Roughness Progression on Kansas Portland Cement Concrete (PCC) Pavements, *Final Report K-Tran: KSU-00-6*, Department of Civil Engineering, Kansas State University, Manhattan, KS, USA.
24. Selezneva, O., Jiang, J., and Tayabji, S.D., (2000). Preliminary Evaluation And Analysis Of LTPP Faulting Data - Final Report, *FHWA-RD-00-076*, *FHWA,* Washington D. C., USA.
25. Liu, C. and Gazis, D.C., (1999). Dynamic Surface Roughness Effect on the Response of a Pavement Structure, *J. Transp. Eng.*, **125**(4), pp. 332-33.
26. Liu, C., (2001). Pavement Response to Moving Loads, *International Journal of Road Materials and Pavement Design,* **2**(3), pp. 263-282.
27. Cebon, D., (1999). Handbook of Vehicle-Road Interaction, Swets & Zeitlinger Publisher, Lisse, the Netherlands.
28. Liu, C. and Herman, R., (1997). Roadway-Vehicle Interaction, Physical Indexes, and Human Judgment of Ride Quality, *Transportation Research Record, No. 1570***,** pp. 55-59.
29. Federal Highway Administration (FHWA), (2000). Preliminary Evaluation and Analysis of LTPP Faulting Data-Final Report, *FHWA-RD-00-076*, USDOT, Washington D.C., USA.
30. Federal Highway Administration (FHWA), (2003). Product Brief-Pavement Viewer and Analyzer, *FHWA-RD-03-070*, USDOT, Washington D.C., USA.